On the Implementation of Novel Velocity-based 3D Beam: Compatibility of Angular Velocities Over the FEM Boundaries

Eva Zupan and Dejan Zupan

Faculty of Civil and Geodetic Engineering
University of Ljubljana
Ljubljana, Slovenia
Email: eva.zupan.lj@gmail.com; dejan.zupan@fgg.uni-lj.si

***Abstract*—In this paper, a new velocity-based finite element approach for non-linear dynamics of beam-like structures is briefly introduced. The additivity of angular velocities in local frame description, which are taken as primary unknowns along with the linear velocities, brings several benefits, such as trivial discretization and update procedure for the primary unknowns and improved stability properties of the time integrator. The novel approach introduces some new issues that need to be treated properly, such as compatibility of angular velocities over the finite element boundaries. A computationally cheap solution of the problem is presented.**

Keywords–non-linear dynamics; spatial beams; finite-element method; velocity-based approach;

I. INTRODUCTION

The total set of equations in solid mechanics consists of non-linear equilibrium, kinematic and constitutive equations that need to be solved for displacements, strains and stresses. Many practical problems in solid mechanics deal with structures that have one dimension larger than the other two, e.g., columns and girders in civil engineering, robotic arms, rotor blades and aircraft wings in mechanical engineering, deoxyribonucleic acid (DNA) molecules in biology and medicine, nanotubes in nanotechnology. Such structures are usually modelled as beams. For beam-like structures the kinematics of a body becomes simplified but the equations remain non-linear, see, e.g., Antman [1]. Additionally, the reduced kinematics introduces the three-dimensional rotations of rigid cross-sections to describe the configuration of a beam. The solution algorithms for beams usually reduce the total set of equations in such a way that the configuration variables (displacements and rotations) become the only unknowns of the problem. For numerical solution methods, such reduction means that the configuration variables need to be discretized with respect to space and time. The three-dimensional rotations, which are important members of configuration variables, represent a demanding mathematical structure, characterized by multiplicative nature (non-additivity), orthogonality and non-commutativity. These properties need to be properly considered in the numerical solution methods to gain a sufficient performance of calculations and accuracy of the results. Such demands highly increase the complexity of algorithms and disable direct applicability of the methods developed for standard Euclidean spaces [2]–[5].

The alternative approach employed here exploits computationally simpler angular velocities as the primary quantities for the description of rotational degrees of freedom. Such approach brings several advantages to non-linear beam dynamics:

- when expressed in local bases, the components of angular velocity vector become additive, which enables the use of standard discretization and interpolation techniques;
- the stability of implicit time integrators is improved by taking the derivative of configuration quantities as the iterative unknowns, see Hosea and Shampine [6];
- the time discretization, linearization of equations and the update procedure are much simpler compared to standard beam elements.

Besides the advantages, this new approach brings some novel issues that need to be properly solved. The crucial idea of the finite element method (FEM) lies in subdivision of a larger structure into smaller parts called finite elements. An important part of the solution procedure is the assembly of equations of finite elements into a larger system of equations that describe the problem at the structural level. The simplest assumption used in the assembly procedure is that the elements are rigidly connected so that the displacements and rotations are continuous over the boundaries. When the displacements and rotations are chosen as the primary variables, a simple Boolean identification of degrees of freedom can be used. This yields that velocities and angular velocities are continuous over the finite element boundaries as well, but only when expressed with respect to a fixed basis.

For the sake of computational advantages at the element level, we express the angular velocities with respect to the moving frame. Because of this choice, the simple identification of degrees of freedom that belong to the joints between elements can no longer be used due to different initial orientations of elements. Thus, the continuity of configuration quantities in a fixed frame leads to a more complicated relation in the local frame. This relation could be introduced at the structural level using the method of Lagrange multipliers, but such an approach would increase the number of degrees of freedom and the computational complexity of the overall algorithm. An elegant and computationally cheap alternative is presented here. Excellent properties of the proposed numerical model are demonstrated by numerical examples.

The rest of the paper is structured as follows. Section II introduces Cosserat beam model. In Section III, we describe a novel numerical solution method for Cosserat beams. The treatment of boundary conditions is presented in Section IV. In Section V, some numerical examples are given. The paper ends with concluding remarks.

 ISBN: 978-1-61208-506-7

II. COSSERAT BEAM MODEL

Among beam models, the *Cosserat theory of rods*, [1], is widely used. The numerical implementation of the model is usually attributed to Reissner [7] and Simo [8], where it is also called *the geometrically exact beam*. Only a brief description of the model is presented here.

The centroidal line $\left\{ \vec{r}\,(x,t)\,,\ x \in [0,L]\,,\ t \geq 0 \right\}$ and the family of cross-sections $\{\mathcal{A}\,(x,t)\,,\ x \in [0,L]\,,\ t \geq 0\}$ of the beam are parametrized by the arc-length parameter x and the time t, where L is the length of the beam in its initial position, see Figure 1. We assume that cross-sections are bounded plane regions that preserve their shape and area during deformation.

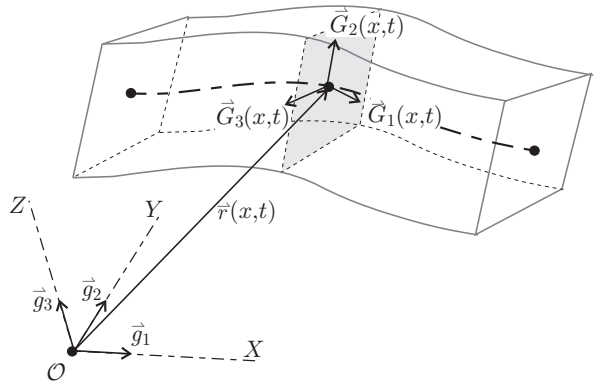

Figure 1. A three-dimensional beam.

For the description of beam equations and the quantities therein, we introduce the *local* orthonormal basis $\left\{ \vec{G}_1\,(x,t)\,, \vec{G}_2\,(x,t)\,, \vec{G}_3\,(x,t) \right\}$, which defines the orientation of each cross-section, and the *global* orthonormal basis $\left\{ \vec{g}_1, \vec{g}_2, \vec{g}_3 \right\}$, which is fixed in time and space. A rotation between the global and the local basis, defined by the quaternion multiplication ($\circ$) reads

$$\vec{G}_i\,(x,t) = \widehat{q}\,(x,t) \circ \vec{g}_i \circ \widehat{q}^{\,*}\,(x,t)\,, \qquad i = 1,2,3, \tag{1}$$

where $\widehat{q}$ denotes the rotational quaternion and $\widehat{q}^{\,*}$ its conjugate.

III. NUMERICAL SOLUTION METHOD

The total set of governing equations describing dynamics of Cosserat rods in terms of quaternions can be found, e.g., in [9] or [10]. Following the classical Galerkin finite-element approach and introducing a family of interpolation functions $I_p\,(x)$, $p = 1,2,...,N$, the discretized balance equations of a beam read:

$$\int_0^L \left[\mathbf{n} I_p' - \tilde{\mathbf{n}} I_p + \rho A \ddot{\mathbf{r}} I_p \right] dx - \delta_p \boldsymbol{f} = \mathbf{0} \tag{2}$$

$$\int_0^L \Big[\mathbf{m} I_p' - (\mathbf{r}' \times \mathbf{n})\, I_p - \tilde{\mathbf{m}} I_p + \widehat{\mathbf{q}} \circ \left(\mathbf{J}_\rho \dot{\boldsymbol{\Omega}} \right) \circ \widehat{\mathbf{q}}^{\,*} I_p + \boldsymbol{\omega} \times \left(\widehat{\mathbf{q}} \circ (\mathbf{J}_\rho \boldsymbol{\Omega}) \circ \widehat{\mathbf{q}}^{\,*} \right) I_p \Big] dx - \delta_p \boldsymbol{h} = \mathbf{0}. \tag{3}$$

The bold-face letters represent vector quantities in the component form. The lower case letters are used when a vector is expressed with respect to the fixed frame and the upper case letters are used for the local basis description. A hat over the letter denotes a four-dimensional vector, a member of the algebra of quaternions. Here, $\mathbf{n}$ and $\mathbf{m}$ are the resultant force and moment vector of the cross-section expressed in fixed frame, i.e.,

$$\mathbf{n}\,(x,t) = \widehat{\mathbf{q}}\,(x,t) \circ \mathbf{N}\,(x,t) \circ \widehat{\mathbf{q}}^{\,*}\,(x,t)\,, \tag{4}$$

$$\mathbf{m}\,(x,t) = \widehat{\mathbf{q}}\,(x,t) \circ \mathbf{M}\,(x,t) \circ \widehat{\mathbf{q}}^{\,*}\,(x,t)\,, \tag{5}$$

where $\mathbf{N}$ and $\mathbf{M}$ are the same vectors expressed in local basis; $\boldsymbol{\Omega}$ and $\dot{\boldsymbol{\Omega}}$ are the angular velocity and angular acceleration; $\ddot{\mathbf{r}}$ is the linear acceleration; ρ is the density of the material; A is the area of the cross-section; $\mathbf{J}_\rho$ is the matrix of mass moments of inertia; $\tilde{\mathbf{n}}$ and $\tilde{\mathbf{m}}$ are vectors of applied distributed force and moment; $\delta_p \mathbf{f}\,(t)$ and $\delta_p \mathbf{h}\,(t)$ are the applied concentrated forces and moments at ends of the beam:

$$\delta_p \mathbf{f}\,(t) \;=\; \begin{cases} \mathbf{f}^0\,(t)\,, & p = 1 \\ \mathbf{f}^L\,(t)\,, & p = N \\ 0, & \text{otherwise} \end{cases}$$

$$\delta_p \mathbf{h}\,(t) \;=\; \begin{cases} \mathbf{h}^0\,(t)\,, & p = 1 \\ \mathbf{h}^L\,(t)\,, & p = N \\ 0, & \text{otherwise} \end{cases} .$$

Equations (2)–(3) represent a system of $6N$ equations discrete in time but still continuous in space. The dependency of quantities on space x and time t has been omitted for better readability. They need to be solved together with kinematic and constitutive equations. Kinematic equations of Cosserat beam are as follows

$$\boldsymbol{\Gamma} = \widehat{\mathbf{q}}^{\,*} \circ \mathbf{r}' \circ \widehat{\mathbf{q}} + \boldsymbol{\Gamma}_0, \qquad \mathbf{K} = 2\widehat{\mathbf{q}}^{\,*} \circ \widehat{\mathbf{q}}', \tag{6}$$

where $\boldsymbol{\Gamma}$ and $\mathbf{K}$ denote the translational strain vector and the shear strain vector, respectively. For constitutive equations various models could be taken, but here we limit ourselves to the simplest case of linear elastic material, where

$$\mathbf{N} = \mathrm{diag}\,[\ EA \quad GA_2 \quad GA_3\ ]\,\boldsymbol{\Gamma} \tag{7}$$

$$\mathbf{M} = \mathrm{diag}\,[\ GI_1 \quad EI_2 \quad EI_3\ ]\,\mathbf{K}. \tag{8}$$

Here, EA/L is the axial stiffness, EI_2 and EI_3 denote the bending stiffness, GI_1/L is the torsional stiffness, GA_2 and GA_3 are the shear stiffnesses.

A. Time discretization

For the time discretization, we use the approximation of displacements at t_{n+1} following from the mean value theorem:

$$\mathbf{r}^{[n+1]} = \mathbf{r}^{[n]} + h \frac{\mathbf{v}^{[n]} + \mathbf{v}^{[n+1]}}{2},$$

which yields

$$\mathbf{r}^{[n+1]} = \mathbf{r}^{[n]} + h \overline{\mathbf{v}},$$

where $\overline{\mathbf{v}}$ denotes the average velocity

$$\overline{\mathbf{v}} = \frac{\mathbf{v}^{[n]} + \mathbf{v}^{[n+1]}}{2}$$

and $h = t_{n+1} - t_n$ is the time step of the scheme.

For accelerations we can similarly employ

$$\frac{\mathbf{a}^{[n]} + \mathbf{a}^{[n+1]}}{2} = \frac{\mathbf{v}^{[n+1]} - \mathbf{v}^{[n]}}{h}.$$

 ISBN: 978-1-61208-506-7

After some rearrangement of terms, the scheme for translational degrees of freedom reads

$$\begin{aligned}\mathbf{r}^{[n+1]} &= \mathbf{r}^{[n]} + h\overline{\mathbf{v}}\\ \mathbf{v}^{[n+1]} &= -\mathbf{v}^{[n]} + 2\overline{\mathbf{v}}\\ \mathbf{a}^{[n+1]} &= -\mathbf{a}^{[n]} - \frac{4}{h}\mathbf{v}^{[n]} + \frac{4}{h}\overline{\mathbf{v}}.\end{aligned} \tag{9}$$

This scheme can be interpreted as a modification of the classical implicit Newmark scheme, where the average velocity becomes the iterative unknown.

A similar approach can be used for rotational degrees of freedom with an important exception stemming from the nonlinear relationship between angular velocities and rotational quaternions. The exponential mapping is used to map from incremental angular velocities to incremental rotations. The incremental rotation is then multiplied with the current one. The scheme for rotational degrees of freedom reads

$$\begin{aligned}\widehat{\mathbf{q}}^{[n+1]} &= \widehat{\mathbf{q}}^{[n]} \circ \exp\left(\frac{h}{2}\overline{\mathbf{\Omega}}\right)\\ \mathbf{\Omega}^{[n+1]} &= -\mathbf{\Omega}^{[n]} + 2\overline{\mathbf{\Omega}}\\ \boldsymbol{\alpha}^{[n+1]} &= -\boldsymbol{\alpha}^{[n]} - \frac{4}{h}\mathbf{\Omega}^{[n]} + \frac{4}{h}\overline{\mathbf{\Omega}},\end{aligned} \tag{10}$$

where exp denotes the quaternion exponential

$$\exp\left(\widehat{\mathbf{x}}\right) = \widehat{\mathbf{1}} + \frac{\widehat{\mathbf{x}}}{1!} + \frac{1}{2!}\widehat{\mathbf{x}}\circ\widehat{\mathbf{x}} + \frac{1}{3!}\widehat{\mathbf{x}}\circ\widehat{\mathbf{x}}\circ\widehat{\mathbf{x}} + ... \tag{11}$$

B. Spatial discretization

In the present time discretization, the average velocities $\overline{\mathbf{v}}$ and $\overline{\mathbf{\Omega}}$ are the only unknown functions along the length of the beam at each particular time step. They are replaced by a set of nodal values $\overline{\mathbf{v}}^p$, $\overline{\mathbf{\Omega}}^p$ at discretization points x_p, $p = 1, \ldots, N$, with $x_1 = 0$ and $x_N = L$, and interpolated by a set of interpolation functions $I_p(x)$ in-between:

$$\overline{\mathbf{v}}\left(x\right) = \sum_{p=1}^{N} I_p\left(x\right)\overline{\mathbf{v}}^p, \qquad \overline{\mathbf{\Omega}}\left(x\right) = \sum_{p=1}^{N} I_p\left(x\right)\overline{\mathbf{\Omega}}^p. \tag{12}$$

The same discretization procedure is performed at every finite element of the structure. Thus, boundary nodes x_1 and x_N become members of the global notes important at the structural level, while x_2,... x_{N-1} are internal points of the element, often but not necessarily condensed at the elements level. Angular velocities in local basis description are additive quantities and the standard aditive-type interpolation used is in complete accord with the properties of the configuration space.

C. Newton iteration

After time and space discretization, the governing equations (2)–(3) are replaced by a set of nonlinear algebraic equations that need to be solved at each discrete time for all the nodal values. The non-linear equations are solved iteratively using the Newton-Raphson method

$$\mathbf{K}^{[i]}\delta\mathbf{y} = -\mathbf{f}^{[i]}, \tag{13}$$

where $\mathbf{K}^{[i]}$ is the global Jacobian tangent matrix, $\mathbf{f}^{[i]}$ the residual vector of discretized equations (2)–(3), both in iteration i, and $\delta\mathbf{y}$ a vector of corrections of all nodal unknowns

$$\delta\mathbf{y} = \left[\begin{array}{cccc}\delta\overline{\mathbf{v}}_1 & \delta\overline{\mathbf{\Omega}}_1 & \cdots & \delta\overline{\mathbf{v}}_M \quad \delta\overline{\mathbf{\Omega}}_M\end{array}\right]^T$$

A suitable choice of nodal variables allows the kinematically admissible additive update:

$$\overline{\mathbf{v}}^{[i+1]} = \overline{\mathbf{v}}^{[i]} + \delta\overline{\mathbf{v}}, \qquad \overline{\mathbf{\Omega}}^{[i+1]} = \overline{\mathbf{\Omega}}^{[i]} + \delta\overline{\mathbf{\Omega}} \tag{14}$$

at each discrete point of the structure.

IV. Continuity of boundary values

Finite elements have equal displacements and rotations at the rigid joints. However, the initial rotations of different elements are not necessarily equal. When the initial orientations differ, we need to distinguish between the initial and the relative rotations. Let us start with two elements having different initial orientations, described by quaternions $\widehat{\mathbf{q}}_0^{\mathrm{I}}$ and $\widehat{\mathbf{q}}_0^{\mathrm{II}}$ at the joint: $\widehat{\mathbf{q}}_0^{\mathrm{I}} \neq \widehat{\mathbf{q}}_0^{\mathrm{II}}$. When the joint is rigid the position vectors are equal, but the total rotations differ

$$\mathbf{r}^{\mathrm{I}} = \mathbf{r}^{\mathrm{II}} \qquad \text{and} \qquad \widehat{\mathbf{q}}^{\mathrm{I}} \neq \widehat{\mathbf{q}}^{\mathrm{II}}, \tag{15}$$

as shown in Figure 2.

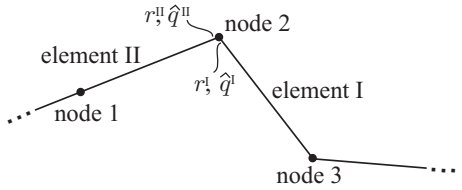

Figure 2. A rigid joint of two differently oriented elements.

The total rotations can be expressed as a composition of initial and relative rotation

$$\widehat{\mathbf{q}}^{\mathrm{I}} = \widehat{\mathbf{q}}_0^{\mathrm{I}} \circ \widehat{\mathbf{k}}^{\mathrm{I}} \qquad \text{and} \qquad \widehat{\mathbf{q}}^{\mathrm{II}} = \widehat{\mathbf{q}}_0^{\mathrm{II}} \circ \widehat{\mathbf{k}}^{\mathrm{II}}, \tag{16}$$

where the relative rotations are equal:

$$\widehat{\mathbf{k}}^{\mathrm{I}} = \widehat{\mathbf{k}}^{\mathrm{II}}. \tag{17}$$

The continuity condition, which could also be called the compatibility of rotations at the element boundaries, thus reads

$$\widehat{\mathbf{q}}^{\mathrm{I}} \circ \widehat{\mathbf{q}}_0^{\mathrm{I}*} = \widehat{\mathbf{q}}^{\mathrm{II}} \circ \widehat{\mathbf{q}}_0^{\mathrm{II}*}.$$

In configuration based approach we usually avoid enforcing this condition by introducing the relative rotational quaternion $\widehat{\mathbf{k}}$ as the nodal variable. For the velocity-based approach, we can similarly observe that

$$\overline{\mathbf{v}}^{\mathrm{I}} = \overline{\mathbf{v}}^{\mathrm{II}} \qquad \text{and} \qquad \overline{\mathbf{\Omega}}^{\mathrm{I}} \neq \overline{\mathbf{\Omega}}^{\mathrm{II}},$$

as the angular velocities are expressed in different local frames. We will derive the compatibility condition for angular velocities at the joints and propose a similar strategy as for rotational quaternions to avoid the use of Lagrange multipliers method by the substitution of the primary unknowns of Newton's iteration at the structural level. The details are presented in the sequel.

A. Relation between boundary angular velocities

The angular velocity vector expressed in the local frame is defined as

$$\mathbf{\Omega} = 2\widehat{\mathbf{q}}^* \circ \dot{\widehat{\mathbf{q}}}, \tag{18}$$

which yields the expressions for the nodal angular velocities of elements I and II at the joint

$$\overline{\mathbf{\Omega}}^{\mathrm{I}} = 2\widehat{\mathbf{q}}^{\mathrm{I}*} \circ \dot{\widehat{\mathbf{q}}}^{\mathrm{I}} \qquad \text{and} \qquad \overline{\mathbf{\Omega}}^{\mathrm{II}} = 2\widehat{\mathbf{q}}^{\mathrm{II}*} \circ \dot{\widehat{\mathbf{q}}}^{\mathrm{II}}.$$

After considering (16), we have

$$\overline{\mathbf{\Omega}}^{\mathrm{I}} = 2\widehat{\mathbf{q}}_0^{\mathrm{I}*} \circ \widehat{\mathbf{k}}^{\mathrm{I}*} \circ \dot{\widehat{\mathbf{k}}}^{\mathrm{I}} \circ \widehat{\mathbf{q}}_0^{\mathrm{I}} \quad \text{and} \quad \overline{\mathbf{\Omega}}^{\mathrm{II}} = 2\widehat{\mathbf{q}}_0^{\mathrm{II}*} \circ \widehat{\mathbf{k}}^{\mathrm{II}*} \circ \dot{\widehat{\mathbf{k}}}^{\mathrm{II}} \circ \widehat{\mathbf{q}}_0^{\mathrm{II}}.$$

Since the relative rotation $\widehat{\mathbf{k}}$ is continuous over the boundaries of elements, eq. (17), we are able to express the constraint relation between the boundary angular velocities

$$\widehat{\mathbf{q}}_0^{\mathrm{I}} \circ \overline{\mathbf{\Omega}}^{\mathrm{I}} \circ \widehat{\mathbf{q}}_0^{\mathrm{I}*} = \widehat{\mathbf{q}}_0^{\mathrm{II}} \circ \overline{\mathbf{\Omega}}^{\mathrm{II}} \circ \widehat{\mathbf{q}}_0^{\mathrm{II}*}. \tag{19}$$

For the clarity of further derivation, it is convenient to express (19) in terms of rotation matrices:

$$\mathbf{R}_0^{\mathrm{I}} \overline{\mathbf{\Omega}}^{\mathrm{I}} = \mathbf{R}_0^{\mathrm{II}} \overline{\mathbf{\Omega}}^{\mathrm{II}}, \tag{20}$$

where $\mathbf{R}_0^{\mathrm{I}}$ and $\mathbf{R}_0^{\mathrm{II}}$ denote the standard rotation matrices equivalent to quaternion-based rotations expressed with $\widehat{\mathbf{q}}_0^{\mathrm{I}}$ and $\widehat{\mathbf{q}}_0^{\mathrm{II}}$.

B. Algorithmically enforced boundary conditions

A solution of two moment equilibrium equations (3) expressed at the same node, here formally written as

$$\mathcal{M}^{\mathrm{I}}\left(\overline{\mathbf{\Omega}}^{\mathrm{I}}\right) = \mathbf{0} \qquad \text{and} \qquad \mathcal{M}^{\mathrm{II}}\left(\overline{\mathbf{\Omega}}^{\mathrm{II}}\right) = \mathbf{0}, \tag{21}$$

needs to be found. The solution must also satisfy the algebraic constraint

$$\mathbf{R}_0^{\mathrm{I}} \overline{\mathbf{\Omega}}^{\mathrm{I}} - \mathbf{R}_0^{\mathrm{II}} \overline{\mathbf{\Omega}}^{\mathrm{II}} = 0. \tag{22}$$

Following the method of Lagrange multipliers the constraint equation is multiplied by a multiplier λ and linearized. The corresponding partial derivatives are then added to the initial variational problem to obtain the weak form of Lagrange function. For the present case it reads

$$\mathcal{M}^{\mathrm{I}}\left(\overline{\mathbf{\Omega}}^{\mathrm{I}}\right) + \mathbf{R}_0^{\mathrm{I}} \lambda = \mathbf{0} \tag{23}$$

$$\mathcal{M}^{\mathrm{II}}\left(\overline{\mathbf{\Omega}}^{\mathrm{II}}\right) - \mathbf{R}_0^{\mathrm{II}} \lambda = \mathbf{0} \tag{24}$$

$$\mathbf{R}_0^{\mathrm{I}} \overline{\mathbf{\Omega}}^{\mathrm{I}} - \mathbf{R}_0^{\mathrm{II}} \overline{\mathbf{\Omega}}^{\mathrm{II}} = \mathbf{0}. \tag{25}$$

The method thus increases the size of the system and the computational demands. It introduces three additional scalar unknowns and three additional equations for each rigid joint between two elements. To avoid this, we introduce the following change of variables describing the nodal rotation-related unknowns:

$$\overline{\mathbf{\Omega}}_R^{\mathrm{I}} = \mathbf{R}_0^{\mathrm{I}} \overline{\mathbf{\Omega}}^{\mathrm{I}} \qquad \text{and} \qquad \overline{\mathbf{\Omega}}_R^{\mathrm{II}} = \mathbf{R}_0^{\mathrm{II}} \overline{\mathbf{\Omega}}^{\mathrm{II}}. \tag{26}$$

Based on the substitution of unknowns (26), the method of Lagrange multipliers gives

$$\mathcal{M}^{\mathrm{I}}\left(\mathbf{R}_0^{\mathrm{I}T} \overline{\mathbf{\Omega}}_R^{\mathrm{I}}\right) + \lambda = \mathbf{0} \tag{27}$$

$$\mathcal{M}^{\mathrm{II}}\left(\mathbf{R}_0^{\mathrm{II}T} \overline{\mathbf{\Omega}}_R^{\mathrm{II}}\right) - \lambda = \mathbf{0} \tag{28}$$

$$\overline{\mathbf{\Omega}}_R^{\mathrm{I}} - \overline{\mathbf{\Omega}}_R^{\mathrm{II}} = \mathbf{0}. \tag{29}$$

The system (27)–(29) can be easily reduced since the nodal unknowns are now identical: $\overline{\mathbf{\Omega}}_R^{\mathrm{I}} = \overline{\mathbf{\Omega}}_R^{\mathrm{II}}$. These new variables can be interpreted as the relative angular velocities in a relative local frame. After the summation of the first two equations, we obtain the reduced moment equilibrium equation at the joint:

$$\mathcal{M}^{\mathrm{I}}\left(\mathbf{R}_0^{\mathrm{I}T} \overline{\mathbf{\Omega}}_R^{\mathrm{I}}\right) + \mathcal{M}^{\mathrm{II}}\left(\mathbf{R}_0^{\mathrm{II}T} \overline{\mathbf{\Omega}}_R^{\mathrm{I}}\right) = 0.$$

Translational degrees of freedom are left unchanged. The correction vector of iteration method thus becomes

$$\delta \mathbf{y}_R = \left[\begin{array}{cccc} \delta\overline{\mathbf{v}}_1 & \delta\overline{\mathbf{\Omega}}_{R,1} & \cdots & \delta\overline{\mathbf{v}}_M \quad \delta\overline{\mathbf{\Omega}}_{R,M} \end{array} \right]^T.$$

Note that the corrections of newly introduced variables (26) can still be directly summed up to the current iterative values. This property follows from the distributivity of multiplication of time-constant matrix $\mathbf{R}_0$ with the sum of angular velocity and its update. The original quantities $\overline{\mathbf{\Omega}}^{\mathrm{I}}$ and $\overline{\mathbf{\Omega}}^{\mathrm{II}}$ remain to be the interpolated quantities at the elements level. Hence in each iteration step i the variables $\overline{\mathbf{\Omega}}^{\mathrm{I}}$ and $\overline{\mathbf{\Omega}}^{\mathrm{II}}$ are extracted from $\overline{\mathbf{\Omega}}_R^{\mathrm{I}} = \overline{\mathbf{\Omega}}_R^{\mathrm{II}}$ and applied for further calculations.

With this procedure only six variables per node are needed and computational complexity is only slightly increased due to reconstruction of average angular velocities at the element's level from the relative ones at the structural level. This procedure is done by applying a simple time-independent rotation. The main advantage, i.e., the additivity of the iterative and the interpolated unknowns, is preserved. The size of the problem for each element thus remains to be $6N$, which means that on the structural level we need to solve $6(N \cdot E - n)$ equations, where E denotes the number of elements and n the number of rigid joints. To enforce the boundary conditions, the proposed method requires additional n matrix products of the initial transposed rotation matrix, $\mathbf{R}_0^T$, and the relative angular velocity, $\overline{\mathbf{\Omega}}_R$. As we will show by numerical example, these costs are negligible with respect to the overall numerical procedure.

V. NUMERICAL STUDIES

The applicability and an excellent performance of the proposed method will be demonstrated on standard examples for flexible beam-like structures with finite strains where the structure undergoes large displacements and rotations. Equidistant discretization points were chosen for spatial discretization and standard Lagrangian polynomials were taken to be interpolation functions. Integrals were evaluated numerically using the Gaussian quadrature rule. The Newton-Raphson iteration scheme was terminated when the Euclidean norm of the vector of corrections of all primary unknowns was under 10^{-9}. The geometric and material data chosen in the examples are

$$\begin{aligned} EA = GA_2 = GA_3 &= 10^6, \\ GI_1 = EI_2 = EI_3 &= 10^3, \\ \rho A &= 1. \end{aligned}$$

Other data are provided for each example separately .

A. Free flight of a beam: the computational performance

In our first example, we analyse the computational performance of the present approach when solving a problem similar to the one introduced by Simo and Vu-Quoc [2]. The beam is initially inclined and subjected to a piecewise linear point force f_X and point moments h_Y and h_Z at the lower end, as shown in Figure 3. The mass-inertia matrix of the cross-section is taken to be: $\mathbf{J}_\rho = \mathrm{diag}\left[\begin{array}{ccc} 10 & 10 & 10 \end{array} \right]$.

For this particular problem, all elements have equal initial orientations. A simple Boolean identification of degrees of freedom is therefore reasonable even if angular velocities in local frame description are the primary unknowns, which is the case in our approach. This allows us to solve the problem

in two different ways: i) with Boolean identification and ii) using the proposed algorithm. By doing so, we will be able to compare the computational times and demonstrate the demands of the presented algorithm. Note that the Boolean identification is not appropriate when solving problems, where elements have different initial inclinations, which limits its applicability and generality.

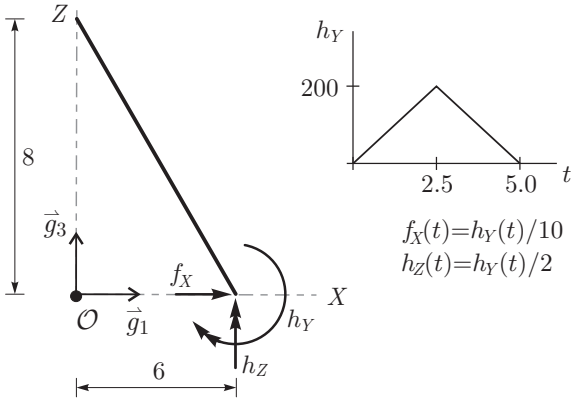

Figure 3. Unsupported beam that is initially straight but inclined.

To compare both methods, a dense mesh of 100 linear elements has been used. For this problem a small number of elements would be sufficient, but by increasing their number the complexity of the overall algorithm raises so the additional demands of the proposed algorithm can be easier observed. The average computational times of the same evaluation in seconds are presented in Table I.

TABLE I. COMPUTATIONAL TIMES OF INITIALLY STRAIGHT BEAM.

Method	*initial time step*	*ten time steps*
Boolean identification	3.415	42.820
proposed algorithm	3.508	34.011

We can observe that computational times of the proposed method are only slightly larger after the first time step. However, in the time stepping procedure the proposed algorithm behaves better since the newly introduced relative velocities seem to be more suitable computational unknowns, which leads to a lower number of total iterations needed and therefore lower computational times.

B. Large deflections of right-angle cantilever

This classical example introduced by Simo and Vu-Quoc [2] was studied by many authors. A right-angle cantilever beam is subjected to a triangular pulse out-of-plane load at the elbow, see Figure 4. Each part of the cantilever is dicretized with two third-order elements. A dynamic responce of the cantilever involves very large magnitudes of displacements and rotations together with finite strains. After removal of the external force, the cantilever undergoes free vibrations and the total mechanical energy of the cantilever should remain constant. Therefore, the stability of the algorithm is here checked through the energy behavior. The centroidal mass-inertia matrix of the cross-section is diagonal: $\mathbf{J}_\rho = \mathrm{diag}\,[\ 20 \quad 10 \quad 10\ ]$. Originally the solution was computed on the time interval $[0, 30]$ with fixed time step 0.25, later the interval was extended to $[0, 50]$ by

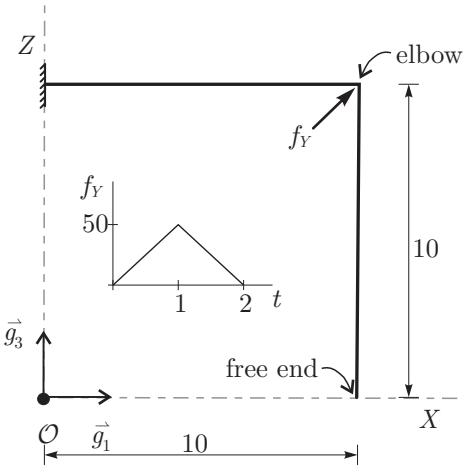

Figure 4. The right-angle cantilever subjected to out-of-plane loading.

Jelenić and Crisfield [11] claiming that most of the algorithms encounter numerical stability problems between times 30 and 50. Here on a longer time interval $[0, 100]$ solution was

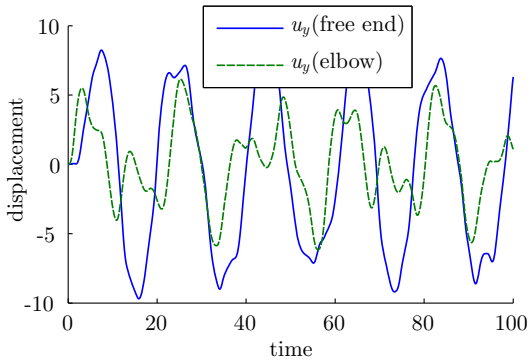

Figure 5. The out-of-plane displacements at free-end and at elbow for the right-angle cantilever.

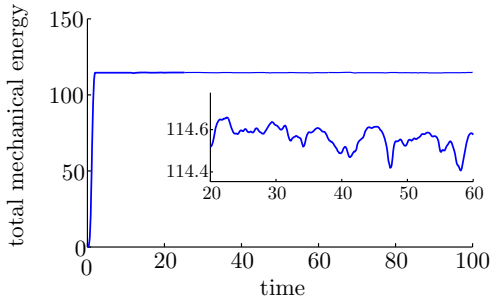

Figure 6. The time history of the total mechanical energy for the right-angle cantilever.

obtained without any numerical problems noticed, see Figure 5. However the time step used had to be reduced by half, $h = 0.125$, otherwise the iteration could not achieve the prescribed tolerance condition at time 51.5. From Figure 6 we can observe almost constant total mechanical energy after

time $t = 5$; only slight discrepancy of about 0.2% can be observed, which indicates good stability of calculations. The present results on the time interval $[0, 30]$ agree well with the results reported by other authors.

C. Large overall motion of a flexible cross-like structure

The large overall motion of completely free "cross" was first presented by Simo et al. [12] to illustrate the performance of the algorithm when calculating the dynamics response of a reticulated structure. The geometry and the applied external out-of plane forces are depicted in Figure 7. The centroidal mass-inertia matrix of the cross-section is taken to be $\mathbf{J}_\rho = \mathrm{diag}\,[\ 10\quad 10\quad 10\ ]$. The solution was computed on a very

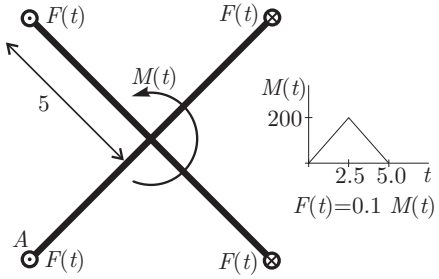

Figure 7. The geometry and the loading of the "cross".

large time interval $[0, 1000]$ with time step $h = 0.1$. Because the interval of calculation is so extremely long we present only displacements on short intervals at the beginning and at the end of calculation, see Figure 8. After removal of external forces at

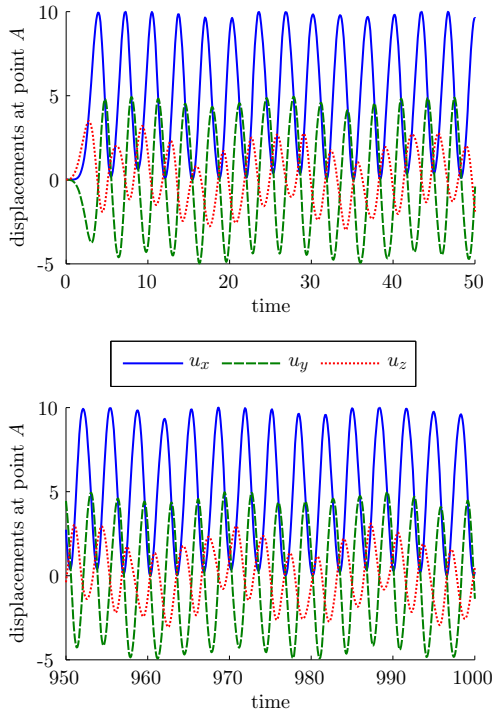

Figure 8. The displacements of the "cross" at point A at the beginning and at the end of calculation.

time $t = 5$ the cross vibrates freely in a periodic-like dynamic

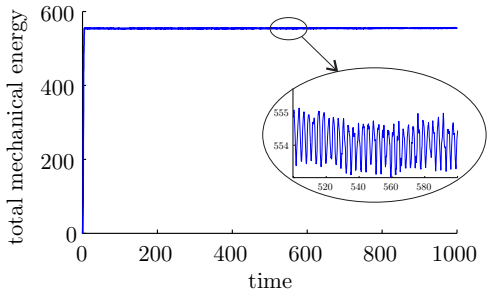

Figure 9. The time history of the total mechanical energy for the "cross".

pattern and the total mechanical energy is almost constant as expected, see Figure 9. The calculations remain stable even after 10 000 time steps.

VI. Conclusion

A novel finite-element approach for the beam dynamics has been presented. The proposed method exploits the benefits of the favourable properties of angular velocity in the local frame description. The issue of the continuity of the structural unknowns over the element boundaries has been resolved with minimal computational cost. The classical benchmark examples demonstrate the accuracy and numerical stability of the proposed method. Its improved behaviour compared to other solution method is evident.

Acknowledgment

This work was supported by the Slovenian Research Agency through the research programme P2-0260. The support is gratefully acknowledged.

References

[1] S. S. Antman, Nonlinear Problems of Elasticity, 2nd ed. Berlin: Springer, 2005.

[2] J. C. Simo and L. Vu-Quoc, "On the dynamics in space of rods undergoing large motions - a geometrically exact approach," Comput. Meth. Appl. Mech. Eng., vol. 66, no. 2, pp. 125–161, 1988.

[3] C. Bottasso and M. Borri, "Integrating finite rotations," Comput. Meth. Appl. Mech. Eng., vol. 164, no. 3-4, pp. 307–331, 1998.

[4] H. Munthe-Kaas, "Runge-Kutta methods on Lie groups," Bit, vol. 38, no. 1, pp. 92–111, 1998.

[5] O. A. Bauchau and S. Han, "Interpolation of rotation and motion," Multibody Syst. Dyn., vol. 31, no. 3, pp. 339–370, 2014.

[6] M. E. Hosea and L. F. Shampine, "Analysis and implementation of TR-BDF2," Appl. Numer. Math., vol. 20, no. 1-2, pp. 21–37, 1996.

[7] E. Reissner, "On finite deformations of space-curved beams," Z. Angew. Math. Phys., vol. 32, no. 6, pp. 734–744, 1981.

[8] J. C. Simo, "A finite strain beam formulation - the three-dimensional dynamic problem. Part I." Comput. Meth. Appl. Mech. Eng., vol. 49, no. 1, pp. 55–70, 1985.

[9] H. Lang, J. Linn, and M. Arnold, "Multi-body dynamics simulation of geometrically exact Cosserat rods," Multibody Syst. Dyn., vol. 25, no. 3, pp. 285–312, 2011.

[10] E. Zupan, M. Saje, and D. Zupan, "Dynamics of spatial beams in quaternion description based on the Newmark integration scheme," Comput. Mech., vol. 51, no. 1, pp. 47–64, 2013.

[11] G. Jelenić and M. A. Crisfield, "Geometrically exact 3D beam theory: implementation of a strain-invariant finite element for statics and dynamics," Comput. Meth. Appl. Mech. Eng., vol. 171, no. 1-2, pp. 141–171, 1999.

[12] J. C. Simo, N. Tarnow, and M. Doblare, "Nonlinear dynamics of 3-dimensional rods - exact energy and momentum conserving algorithms," Int. J. Numer. Methods Eng., vol. 38, no. 9, pp. 1431–1473, 1995.

 ISBN: 978-1-61208-506-7